International Journal of Mass Spectrometry 307 (2011) 112–122

Contents lists available at ScienceDirect

International Journal of Mass Spectrometry

journal homepage: www.elsevier.com/locate/ijms

Imaging of elements and molecules in biological tissues and cells in the low-micrometer and nanometer range

Bei Wu*,[1], J. Sabine Becker

Central Division of Analytical Chemistry, Forschungszentrum Jülich, D-52425 Jülich, Germany

ARTICLE INFO

Article history:
Received 10 November 2010
Received in revised form 14 January 2011
Accepted 18 January 2011
Available online 13 February 2011

Keywords:
Analytical technique
Biological tissue and cell
High spatial resolution
Nano-scale
Nano-scale laser ablation inductively coupled plasma mass spectrometry (LA-ICP-MS)

ABSTRACT

Investigation of small areas of biological tissues or single cells is of particular interest in the life sciences. Chemical imaging in such samples is able to provide the spatial distribution as well as concentrations of elements and molecules present in the sample. At present, the analytical techniques supporting chemical imaging are under intensive development with respect to higher spatial resolution and higher sensitivity and accuracy. In this review, we will focus on the state of the art of advanced mass spectrometric techniques such as secondary ionization mass spectrometry (SIMS), imaging matrix-assisted laser desorption/ionization mass spectrometry (imaging MALDI-MS), nano-scale laser ablation inductively coupled plasma mass spectrometry (LA-ICP-MS) versus non-mass spectrometric techniques, for instance, synchrotron-based X-ray fluorescence and scanning near-field optical microscopy (SNOM) assist Raman spectroscopy, with lateral resolution down to low-micrometer and nanometer scales. The outstanding features and drawbacks of each technique are also discussed regarding their application on the study of biological samples. The promising future of imaging mass spectrometric techniques, especially nano-scale LA-ICP-MS, for application in biochemical studies with high spatial resolution down to the nanometer range is also discussed.

1. Introduction

The distribution and local chemical environment of metals and non-metals in tissues and cells is the most fundamental knowledge of any kind of organism. To obtain information concerning the chemical species, as well as their concentrations and locations is crucial for understanding their biological functions and metabolic process. Traditional solution-based analytical methods require the biological samples to be pre-processed by either digestion or desorption in certain materials for chemical degradation. However, the sample preparation steps may disturb the structure and *in vivo* nature of the tissues and cells. In addition, foreign contamination may occur resulting in difficulties in interpreting of the analytical data. Therefore, there is a need to acquire the chemical information directly from the original biological samples. Bioimaging of elements and molecules in tissues and cells thus becomes necessary for this purpose.

In recent years, there has been a growing interest in the development of analytical techniques for chemical bioimaging, and, indeed, different analytical approaches have been established for directly imaging chemicals in biological samples. These techniques include mass spectrometric methods such as laser ablation inductively coupled plasma mass spectrometry (LA-ICP-MS) [1–4], secondary ionization mass spectrometry (SIMS) [5–8], imaging matrix-assisted laser desorption/ionization mass spectrometry (imaging MALDI-MS) [9–11], synchrotron-based X-ray fluorescence spectroscopy (SR-XRF) [12–15] and synchrotron-based X-ray absorption spectroscopy (SR-XAS) [16–18] (as well as XRF from laboratory X-ray source with relatively lower energy), microscopy techniques based on vibration spectroscopy, for example infrared spectroscopy [19,20] and Raman spectroscopy [21,22], probe-specific detection methods such as confocal fluorescence imaging (CF) via the measurement of fluorescence-labeled molecules [23,24], as well as some hyphenated techniques like scanning or transmission electron microscopy with energy-dispersive X-ray analysis (SEM–EDX or TEM–EDX) [25–27], and so on. Table 1 summarizes the main characteristics of the major bioimaging techniques mentioned above to compare their performances in different applications. Specifically, Fig. 1 gives an overview of the ion sources in mass spectrometric techniques currently used for chemical imaging in the field of life sciences.

In the case of chemical analysis in smaller-size samples such as single cells, sensitive analytical techniques with much higher spatial resolution down to the low-micrometer and even nanometer ranges are required. One strategy is to decrease the size of the

* Corresponding author. Tel.: +49 2461 615163; fax: +49 2461 612560.
E-mail address: b.wu@fz-juelich.de (B. Wu).
[1] Alexander von Humboldt postdoctoral research fellow.

1387-3806/$ – see front matter © 2011 Elsevier B.V. All rights reserved.
doi:10.1016/j.ijms.2011.01.019

Table 1
Comparison of chemical imaging techniques for biological tissues and cells in low-μm and -nm ranges illustrated in this review (a more detailed comparison or characteristics of other techniques can be found in Refs. [7,28]).

Technique	Light source	Detection	Vacuum requirement	Sensitivity	Lateral resolution	Information obtained	Limitation	Examples of application in reference
SIMS	Primary ions	Secondary ions	Yes	>ng g^{-1}	10 μm–50 nm (LMIG: <50 nm)	Element and molecular (1–200 Da)	Strong matrix effects, difficult to quantify	[35,38]
Imaging MALDI-MS	Laser	Pseudomolecular ions	Yes	μg g^{-1}	150–20 μm (7 μm in Ref. [46])	Molecular (up to 100 kDa)	Suitable matrix	[52,53]
NF-LA-ICP-MS	Laser	Neutrals post-ionized in ICP	No	>ng g^{-1}	Low-μm down to ~200 nm	Element and isotope (6–250 Da)	Commercial instrument not available	[70–73]
LMD-ICP-MS	Laser	Neutrals post-ionized in ICP	No	μg g^{-1}	Low-μm down to ~300 nm	Element and isotope (6–250 Da)	Laser power	[75]
Aperture SNOM-LA-ToF-MS	Laser	Ionized molecules	No	μg g^{-1}	Low-μm down to ~300 nm	Molecular	Super sensitive MS required for tiny amount of material ablated	[65,67]
Aperture SNOM-Raman	Laser	Raman scattering	No	μg g^{-1}	~100 nm	Molecular	Weak Raman scattering	[106,107]
TERS	Laser	Raman scattering	No	μg g^{-1}	~100 nm	Molecular	Heating of the tip and the sample	[119,120]
μ-XRF	X-ray from SR	X-ray fluorescence	No	0.1 μg g^{-1}	25 μm–50 nm	Element	Access to SR beamline	[88–91]
μ-XAS (XANES)	X-ray from SR	X-ray fluorescence	No	>μg g^{-1}	<100 μm	Oxidation state	Access to SR beamline, references for complex bio-samples	[96,97]

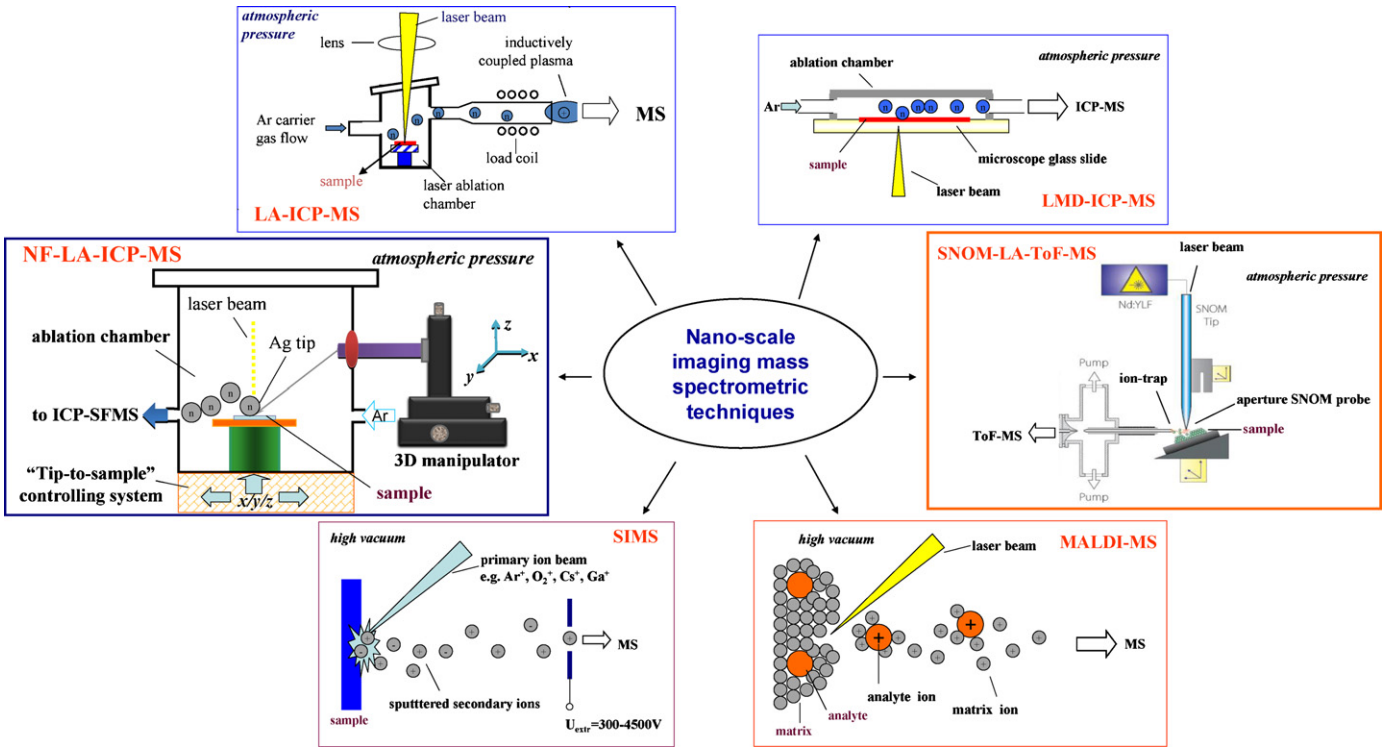

Fig. 1. Ion sources in mass spectrometric techniques currently used for chemical imaging in the field of life sciences. (The figure of SNOM-LA-ToF-MS is reproduced from Ref. [67].)

focused beam used in these techniques. However, a smaller spot size certainly results in smaller amount of material available for analysis, whereas the detection limits of these techniques would be challenged due to the lack of sensitivities from such a small amount of analyte. Another approach is to utilize the physical basis similar to that used in nano-structure imaging techniques, however, without chemical information on the sample surface, such as atomic force microscopy (AFM), scanning tunneling microscopy (STM), as well as scanning near-field optical microscopy (SNOM), to obtain high lateral resolution down to the nanometer range by breaking the optical diffraction limit ($\sim\lambda/2$) into the near-field region. Since there are several excellent reviews with respect to the imaging techniques in the study of biological tissues and cells [28–31], in the present review, we will focus on recent developments in mass spectrometric methods in the direction of nano-range imaging of elements and molecules to come to terms with future challenges in characterizing small tissues and cells with high lateral resolution. Additionally, synchrotron-based XRF and Raman spectroscopy with spatial resolution at nanometer scale will also be discussed for comparison.

2. Nano-scale mass spectrometric techniques

2.1. Nano-secondary ion mass spectrometry (nano-SIMS)

Secondary ion mass spectrometry (SIMS) is currently one of the most important mass spectrometric techniques for surface analysis with respect to depth profiling and element and molecular imaging in the mass range from 1 to 2000 Da. In SIMS, a focused primary ion beam (e.g., Cs^+, O^-, Ga^+, etc.) with high ion energy in a high vacuum ion source is used for sputtering the sample surface materials during bombardment. The sputtered positively and negatively charged secondary atomic and polyatomic ions are then transferred and analyzed by a double-focusing sector field mass spectrometer (SFMS), time-of-flight mass spectrometer (ToF-MS) or quadrupole-based mass spectrometer (QMS) [1]. The development of the primary ion source has improved the spatial resolution in SIMS. The Cs^+ primary ion beam in a dynamic SIMS can be tightly focused as low as 30 nm, while a tightly focused ion beam (<50 nm) with moderate intensity can be produced by the liquid metal ion gun (LMIG) [32]. For molecular analysis, however, it is rather difficult to reach high lateral resolution (normally within the low-μm range), since in static SIMS a defocused ion beam is used in order to keep the molecule at its high m/z ratio. Recently, cluster or polyatomic ion sources, for instance C_{60}^+, Au_n^+ and Bi_n^+, have been developed for use as the primary beams to delivery high energy to the sample surface resulting in the desorption of intact compounds with low damage induced by bombardment as well as high ion yields [33,34]. Using 25 keV Au_3^+ primary ions in ToF-MS (from ION-TOF GmbH, Münster, Germany), which have been implemented in SIMS especially for the measurement of molecular species such as proteins with high molecular weights, imaging of biomolecules (e.g., cholesterol and phospholipids) in mouse brain tissue sections has achieved high spatial resolution as good as ~1 μm [35]. Spatial resolution down to the nanometer range can be reached using now developed instruments of NanoSIMS. A commercial NanoSIMS 50L routinely achieves a lateral resolution of down to 50 and 150 nm with Cs^+ and O^- used as the primary ion sources, respectively [1,36]. By using a double-focusing SFMS with a simultaneous multiple ion collector arrangement, a precise elemental and isotopic analysis with a spatial resolution of 50–200 nm and high sensitivity can be routinely achieved in nano-SIMS with, for example, NanoSIMS 50 and NanoSIMS 50L from CAMECA Instruments (Cameca, Courbevoie, France) [1]. More detailed instrumentation and characteristics of this technique and its application in life sciences can be found in an earlier review by Heeren et al. [37].

One of the first applications of direct imaging SIMS for biological studies can be dated to 1982, when Chandra and co-workers [38] carried out a fundamental study on the gravity-sensing mechanism

of plant roots by investigating calcium location in the amyloplasts of root-cap cells using ion microscope, with the lateral resolution of 1 μm. Subsequently, applications of nano-SIMS in tissue and cell biology [39–42], as well as the interface between organisms and their environment [43,44], have been growing rapidly. Based on SIMS, a mass spectrometric method for imaging isotopes has been developed by Lechene and co-workers to study biological materials, which combines a new generation of SIMS instruments with sophisticated ion optics, labeling with stable isotopes, and quantitative image-analysis software [45]. The new instrument allows the precise and reproducible measurement of isotope ratios via imaging several isotopes simultaneously with high lateral resolution down to 33 nm [45]. By using this method, nitrogen fixation by individual bacteria within eukaryotic host cells has been directly imaged and measured to demonstrate that fixed nitrogen is used for host metabolism [46]. However, the SIMS method only allows analysis under high vacuum conditions, which has limitations for the study of native living cells. Therefore, reliable sample preparation for SIMS analysis is a crucial step with respect to maximum preservation of real information in a biological sample [47]. A comprehensive review of SIMS applications in biological research by Boxer et al. is recommended in Ref. [6]. Recently, we combined two imaging mass spectrometric methods, SIMS and LA-ICP-MS, to generate both elemental and molecular distributions in native cryosections of mouse heart [7]. The results from both spatially resolved imaging techniques were comparable regarding K and Na distribution in the heart slices. In addition, a relation between non-metal (e.g., P) elemental distribution and molecular (e.g., phosphocholine) distribution has been established based on the images of P measured by LA-ICP-MS and phosphocholine images measured by SIMS. However, compared to LA-ICP-MS, the quantification of SIMS data is rather difficult because of the strong matrix dependence of the ion yields and a high formation rate of polyatomic ions [48].

2.2. Imaging matrix-assisted laser desorption/ionization mass spectrometry

Matrix-assisted laser desorption/ionization mass spectrometry (MALDI-MS) is nowadays one of the most important organic mass spectrometric methods used for the analysis of large biomolecules including proteins, peptides and polymers. The sample material is first mixed with a light-absorbing matrix solution containing small organic molecules that have a strong absorption of photons at the laser wavelength [1]. The matrix molecules are in surplus compared to the sample molecules in order to isolate the analyte completely and to absorb the photon energy of the laser beam. The laser power density in MALDI-MS is 2–3 orders of magnitude lower compared to that in LA-ICP-MS in order to produce intact molecular ions that have high molecular weight. The desorption is performed on the dried sample-matrix surface, however, in a high vacuum ion source, to form the aggregate state of the matrix and analyte molecules and thus to change to gaseous phase. The matrix molecule which carries the analyte molecule absorbs most of the incident photon energy to become ionized and simultaneously to avoid the fragmentation of the analyte molecule induced by laser irradiation. This ionization process takes place gently owning to the assistance of the matrix molecules. The intact analyte ions are then extracted in the ion separation system and analyzed by a mass spectrometer [1].

Similar to the liquid sample analyzed by MALDI-MS, in order to image a solid biological tissue or cell by MALDI-MS, the sample surface is required to be covered with an organic compound as the matrix to assist the laser-induced desorption and ionization of the analyte molecule. In imaging MSLDI-MS, the analysis parameters are optimized with respect to high efficiency of desorption and ionization as well as high sensitivity with better spatial resolution. A well-focused laser beam (down to 7 μm [49]), a suitable matrix pattern on the sample surface, and appropriate sample preparation are found to be useful to improve the performance of imaging MALDI-MS [49–52]. Another approach by means of oversampling with complete sample ablation enables the chemical images to be acquired with a resolution higher than the limitations imposed by the size of the laser beam size [53]. The spatial resolution of imaging MALDI-MS on a solid sample can be achieved down to several sub-μm by different approaches [50]. On the other hand, the mechanism of ion formation in the case of such small laser spot sizes has been studied, providing the information on methodological optimization [54]. A protein microscope consisting a combination of scanning near-field optical microscopy (SNOM, see Section 2.3 for the details) and MALDI-MS, has been proposed by Vertes and co-workers [55]. A SNOM probe is placed in the vicinity of the sample surface to raster the tip over the sample at atmospheric pressure. In the case of biological samples, an infrared laser is used as the illumination radiation, and the water content of the sample acts as the matrix. The proposed protein microscope is intended to identify peptides, proteins and other biomolecules within a tissue or cell and to analyze their activity *in vivo*, as well as to provide information on their spatial and temporal distribution down to sub-μm resolution.

2.3. Near-field laser ablation/ionization mass spectrometry combined with the scanning near-field optical microscopy (SNOM) method (SNOM-LA-MS)

As a form of scanning probe microscopy (SPM), scanning near-field optical microscopy (SNOM) is a microscopic technique for the investigation of the sample surface on the nano-scale. By exploiting the properties of evanescent waves by placing a light source or a detector in close proximity to the sample surface (optical near field), SNOM overcomes the far-field optical diffraction limit ($\sim\lambda/2$) [56–58]. With this technique, the resolution of the image is only limited by the detector dimension and not by the wavelength of the illuminating light. SNOM can be operated in both an aperture and an apertureless mode. Aperture SNOM utilizes a sharpened metal-coated optical fiber to allow the illuminating light to pass through the very small aperture at the end of the fiber onto the sample surface with a spot much smaller than the diffraction limit, while apertureless SNOM makes use of a sharp metallic tip inserted in the radiation near-field to form the evanescent near-field radiation. Compared to apertureless SNOM, which is more complicated theoretically and in operation, aperture mode SNOM is currently more popular in application, although there are many issues associated with the aperture tips, for instance, heating, artifacts, contrast and sensitivity.

The aperture tip in SNOM is normally prepared by either pulling or chemical etching of an optical fiber to form a tapered tip, which is then metalized with, for example, Al [59–61]. The prepared tip can vary in shape and diameter from several tens to hundreds of nanometer. Zenobi's group at ETH Zürich [61] has developed a self-determinating process called "tube-etching" to yield tips with a tip apex of 70–200 nm and a high optical transmission which is 2–4 orders of magnitude higher than that of conventional pulled fiber tips. This method was found to be highly reproducible and efficient to produce high-definition near-field optical probes with large cone angles and smooth, sidehole-free aluminum coatings [61,62]. The aperture probe works as a nanolight source, creating craters with a lateral resolution of 70 nm on the sample surface [63].

With the combination of SNOM and the chemical analysis method, both the topography and chemical information of the sample surface can be obtained with nanometric spatial resolution. As early as 1998, Kossakovski and co-workers [64] developed an instrument for simultaneous surface topographical and chemical

analysis by coupling a SNOM probe with a time-of-flight mass spectrometer (ToF-MS). The UV laser radiation was delivered by the uncoated SNOM probe which was located in a vacuum chamber to the sample surface and induced laser desorption and ionization of the sample materials which were then transported and analyzed by the ToF-MS. The mass spectra of the dried acetylcholine (ACh) and dihydroxybenzoic acid (DHB) droplets on a copper plate have been obtained. The spatial resolution of line scan was estimated to be 1 μm.

In 2001, Zenobi's group [65] combined the SNOM probe with a quadrupole mass spectrometer (QMS) for the laser ablation of organic compounds. The optical probe had a 170-nm-diameter aperture, which guided a pulsed laser to the sample surface to create a laser ablation crater of about the same diameter. The laser ablation was carried out at atmospheric pressure using a nanosampling interface with a heated stainless steel capillary orifice called ion-trap positioned very close (<5 μm) to the SNOM probe, in order to suck in the tiny amount of ablated material and transport it into the ion source of the mass spectrometer. The craters after laser ablation with a spatial resolution of less than 200 nm and a depth of 20 nm were demonstrated. Assuming an energy of 2 nJ exiting the tip and a crater on the sample bis(triazene) with such a dimension, a quantity of ~1.7 attomole of organic substance was ejected to give enough sensitivity for the measurement in the mass spectrometer. The authors attributed the yield of craters to photochemical decomposition rather than a photothermal mechanism due to the detection of products by the mass spectrometer that appeared only a short period (~20 ms) after the laser trigger.

An atmospheric pressure sampling interface for ion-trap/time-of-flight mass spectrometry (IT-ToF-MS) has been developed by the same research group [66] and applied in the SNOM mass spectrometric analysis of organic samples such as solid 2,5-dihydrobenzoic acid, anthracene and pyrene [67]. An aperture SNOM tip coated with Al and Cr with a relatively large aperture size (500–800 nm) was used to lead through the Nd:YLF UV laser (349 nm, <15-ns nominal pulse width, repetition rate of up to 2 kHz) onto the sample surface. The laser ablation took place in the optical near field on the sample surface at atmospheric pressure. The ablated materials were sampled with a heated capillary placed at a distance of 25–100 μm from the ablation spot and transported into the ion-trap for ionization and then analyzed by the ToF mass spectrometer. Topographical images of the sample were recorded by scanning the SNOM tip in shear-force feedback over the sample before and after the laser ablation. With such an arrangement, near-field laser ablation MS at atmospheric pressure with full mass spectral information was shown for the first time with a lateral resolution on the low-micrometer scale (~5 μm). The authors demonstrated that different laser ablation conditions resulted in different craters on the sample surface. Redeposition of the ablation materials on the sample surface has been observed. This invokes the question of how much of the ablated material was efficiently transported to the mass spectrometer. Following this work, using scanning electron microscopy, it was found that as much as 70% of the ablated material could be deposited on the surface of the near-field tip [68]. A fundamental insight into the propagation of the ablated materials was obtained by using uncoated tips on the sample surface of anthracene and tris(8-hydroxyquinolinato)aluminum (Alq_3) pellets. Most material in the near-field ablation plume stopped at a height of around ~50 μm from both the anthracene and Alq_3 surface. Although the tilted sample surface angled at 60° was quite bigger than in the previous study (15°) [67], the results showed that the direction of the near-field ablation plume was neither towards the direction of the surface normal nor towards the axis of incident laser beam, but was deflected further away from the surface normal, opposite to the direction of the incoming laser direction. The finding illustrated the relatively low transport efficiency and low sensitivity of the mass spectrometer, suggesting that the geometry of the near-field laser ablation set-up, with respect to relative positioning between the sampling capillary, the SNOM tip and the sample surface should be further adapted.

Although laser ablation mass spectrometry coupled with aperture mode SNOM has become established in low-μm spatial resolution, it has hardly improved the detection limit of the analyte measured by the mass spectrometer, due to the inherent character of the instrumentation—the smaller spot size resulting from the SNOM tip produces a smaller of material available for analysis, not to mention the fact that there is additional mass loss in the processes of ionization and transportation. It has been estimated that the amount of material from a laser ablation crater in the 100 nm–1 μm diameter range is in the order of a few attomoles to a few femtomoles, depending on the material and laser ablation depth [67]. Therefore, a very high sensitivity mass spectrometer is required to analyze the materials ablated by SNOM-laser ablation.

2.4. Near-field laser ablation inductively coupled plasma mass spectrometry (NF-LA-ICP-MS)

In order to overcome the drawbacks in near-field laser ablation with aperture mode SNOM, an improvement of experimental arrangement can be realized by using an apertureless tip instead of the aperture SNOM probe. The idea is based on the physical principles of near-field optical enhancement, which were illustrated in more detail in our previous publications [69,70]. In general, a very sharp apertureless tip electrochemically etched from a silver wire is brought to the "near-field region" from the surface. The tip functions as a source of secondary evanescent near-field radiation, which can be much more intensive than the field of the primary beam, causing local laser-induced surface effects (e.g., local desorption or ablation of sample) limited only by the object size rather than by diffraction effects. The field enhancement can be expected by 10^4 for a probate spheroid or a long sharp Ag tip. Therefore, the amount of the ablated materials is increased due to the enhanced radiation field and promisingly sufficient for the analysis by mass spectrometer.

In our lab at Forschungszentrum Jülich, we utilize the near-field effect in laser ablation inductively coupled plasma mass spectrometry (LA-ICP-MS) as an atomic mass spectrometric technique, since the technique using inductively coupled plasma mass spectrometry (ICP-MS) with an atmospheric pressure ion source coupled to a suitable laser ablation system (LA) for the direct analysis of solid samples is widely commercially available and is also well established [1,70]. A schematic of the near-field LA-ICP-MS is shown in Fig. 2. To realize the near-field LA-ICP-MS, a thin Ag tip with a tip apex of ≤200 nm is inserted in the radiation field of a defocus laser beam (Nd:YAG laser, wavelength 532 nm) and brought close to the sample surface. Near-field laser ablation is carried out in a small-volume chamber at atmospheric pressure. The ablated materials are transported by Ar as carrier gas into the inductively coupled plasma (ICP) ion source of the sensitive double-focusing sector field mass spectrometer with reverse Nier–Johnson geometry.

By means of single-shot analysis on 2D-gels and biological samples, the possibility was demonstrate for the first time of applying nano-local analysis of biological samples using the near-field effect in LA-ICP-MS with spatial resolution in the hundreds of nanometer ranges [70]. It was observed that due to the near-field effect when the needle is close to the surface, the measured U ion intensity was increased by a factor of 60 in a single laser shot measurement in comparison to transient background signals. In isotope ratio measurements of Cu and Zn in gels doped with enriched ^{65}Cu and ^{67}Zn isotopic tracers, significant enhancements of ^{65}Cu and ^{67}Zn signals were observed. Furthermore, the possibility of quantification in NF-LA-ICP-MS was investigated by isotope ratio measurements using

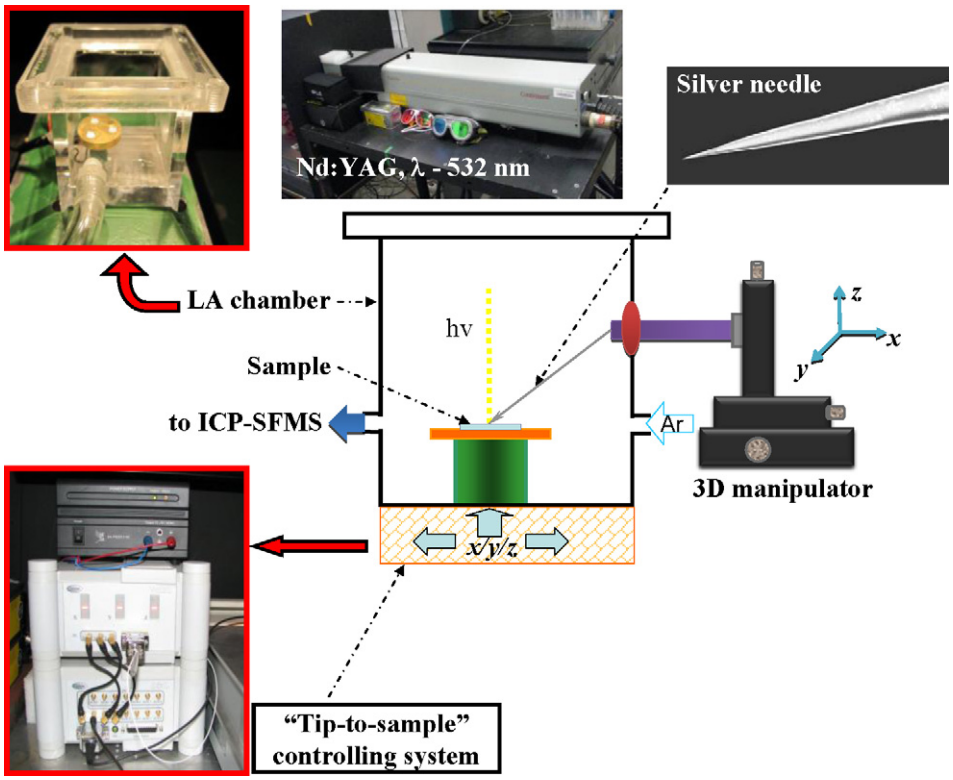

Fig. 2. Schematic of the near-field LA-ICP-MS.

(Revised from Refs. [69,70].)

the biological samples either doped with isotope standard reference material NIST U020 or enriched ^{65}Cu and ^{67}Zn tracers. Both results showed that the quantification procedures in NF-LA-ICP-MS could be carried out via a standard calibration curve and by using the isotope dilution technique.

Since the near-field enhancement effect depends on the shape and diameter of the Ag tip, the positioning of the needle on the surface and the distance between the Ag tip and sample surface, it is crucial to establish a reproducible method for the yields of the Ag tips, as well as a fine controlling system to precisely adjust the tip to the sample surface. Therefore, we developed an electrochemical etching procedure using a droplet of citric acid as the electrolyte in an electrochemical cell to produce a clean Ag tip with a diameter in the range of hundreds of nanometer for use in NF-LA-ICP-MS [71]. For the precise control of the distance between tip and sample surface, a controlling system adapted from an STM system (Anfatec Instruments AG, Oelsnitz, Germany) was developed. This system can be operated in either STM mode by measuring the tunnel current between the tip and the conductive sample surface, or in a dynamic non-contact (DNC) mode by monitoring the amplitude of the oscillating current produced by oscillation of the tip at a fixed frequency which is especially used in the analysis of non-conductive samples like biological tissues and cells. In NF-LA-ICP-MS analysis, one therefore has the option of switching between these two modes according to the character of the sample surface.

In the following studies, the figures of merit of the NF-LA-ICP-MS procedure, including the effect of the tip diameter and the distance between tip and sample on the near field enhancement, were further explored by NF-LA-ICP-MS measurements on various samples such as Au film deposited onto a Si substrate [71], copper isotopic standard reference material, tungsten–molybdenum alloy standard reference material [72] and nanoelectronic devices [73].

By adjusting the DC voltage applied to the electrochemical cell, the thin needle tips can be produced with different diameters. Therefore, we used these tips for the study of resulting laser craters after the NF-LA-ICP-MS measurements [71,72]. We found that the laser craters in range from 200 nm to about 2 μm were produced as a function of the tip diameter of the thin silver needle and the "tip-to-sample" distance [71,72]. During the NF-LA-ICP-MS measurement the needle was controlled by a 3D-manipulator and then by the controlling system via measuring the tunnel current when it was close to the surface. The defocused laser beam did not cause any ablation of the sample material when the needle was far away from the surface. Only background signals were measured in this case. However, a strong increase of ion intensity of the analyte was recorded when the tip of the Ag needle was positioned in the vicinity above the sample surface as the result of near field enhancement effect. Note that, in the case of the measurement of Au-covered Si material, not only the transient signal of $^{197}Au^+$ was shown to have increased about 16-fold, but also the signal of $^{28}Si^+$ was clearly detected while without the near field effect only the background of Si was observed [71]. Within the "near field" region, the distance dependence of the enhancement was studied. The needle tip was placed at 1 nm, 5 nm and 10 nm to the surface of the interdigitated electrode array chip (IDA chip). It was found that at the smaller "tip-to-sample" distance (in the range of 10–1 nm) a higher analyte ion intensity, as well as a larger ablation volume, was observed [72]. However, no Ag signals were observed in any of the NF-LA-ICP-MS measurements, indicating that the near-field enhancement took place selectively on the sample surface [73].

The advantage of using inorganic mass spectrometry is that one can apply isotopic measurements to determine precise and accurate isotopic abundances and isotope ratios in various fields to study the composition of samples and the fate of elements [1]. Therefore, isotope ratios were analyzed in the standard reference materials. Apart from the enhancement of ion intensities measured by ICP-MS, the NF-LA-ICP-MS can precisely determine the isotope ratios of a given element. The average $^{65}Cu^+/^{63}Cu^+$ isotopic

ratio was determined to be 0.4530 on copper isotopic standard reference material NIST SRM 976, giving the relative standard deviation (RSD) of the measurements as low as 3.9%. The isotope ratios of $^{183}W^+/^{184}W^+$ and $^{96}Mo^+/^{98}Mo^+$ with high melting points were measured in good agreement with their listed values of 0.4658 and 0.6929, respectively [72].

With respect to the detection efficiency of the NF-LA-ICP-MS developed here, the theoretical calculation gave a value of 2.7×10^{-5} cps per ablated atom based on a typical laser crater with a diameter of 600 nm on a Au-covered (20 nm in thickness) Si material [72]. Although this is relatively lower than the detection efficiency of conventional LA-ICP-MS, the enhanced signals were sufficient for detection by the sensitive double-focusing sector field ICP-MS with good sensitivity. Similar to the phenomenon observed in SNOM-laser ablation mass spectrometry [67], some particles from the ablated materials were found to be redeposited around the craters. This could be responsible for the fact that less material was transported into the ICP-MS [72]. Nevertheless, the process of near field laser ablation and the material transport should be further studied to obtain full fundamental knowledge about NF-LA-ICP-MS.

Since the NF-LA-ICP-MS has proved to be successful in single-shot measurements, we are currently developing a new experimental arrangement by the implantation of a 3D-movement piezo under the sample holder, together with an improved needle auto-approaching control. The new system will allow us, operated in the DNC-mode of the "tip-to-sample" controlling system, to carry out elemental imaging in biological samples with a spatial resolution on the nanometer scale.

2.5. Laser microdissection inductively coupled plasma mass spectrometry (LMD-ICP-MS)

An alternative concept for nano-scale LA-ICP-MS is proposed by Becker and Salber [74] of introducing a laser microdissection (LMD) apparatus with a powerful solid-state laser into the sample introduction system for a sensitive ICP-MS [75]. The commercialized LMD is based on a microscope technique under direct microscopic visualization using a tightly focused pulse laser or continuous-wave laser beam to isolate individual tissue or cell types from embedded, frozen or fresh biological sections. The complex heterogeneous tissue with the section of interest is placed on a thin polymer foil, or directly on the microscope glass slide without this foil [76]. The polymer foil assists in forming a plasma-mediated ablation initiated by linear absorption [77]. However, direct ablation of the materials through a suitable glass slide without a matrix assistant has already been developed and is available in the commercial LMD. There are numerous applications of LMD serving as a sample preparation method for subsequent multiplex molecular analysis in studies of protoplast, chromosome, whole single cells or cell groups, neurons, and so on, in the life sciences [78–80]. Apart from the further analysis of the dissected sections with respect to proteomic and genomic studies, there is a possibility to directly use the laser beam to ablate the sample materials to obtain elemental and isotopic information within the area if coupled to a sensitive mass spectrometer. In 2005, Hutchinson [81] reported the combination of LMD with LA-ICP-MS as an alternative strategy for the microanalysis of immunohistochemical sections. A laser beam with a spot size of 30 μm was used to cut off Alzheimer's plaques and nonplaque materials of 30–100 μm in diameter and about 5 μm in thickness, but the materials were then analyzed with LA-ICP-MS by line raster to produce elemental responses for Mg, Al, Ca, Fe, Cu and Zn. Recently, for the first time we demonstrated the potential of directly using LMD (SmartCut Plus LMD, MMI Molecular Machines and Industries, Zurich, Switzerland) as a micro-sampling system directly for a sensitive quadrupole-based mass spectrometer with hexapole collision cell (XSeries2, Thermo Fisher Scientific, Bremen, Germany) for imaging elements in small-sections of tissues and cells with high lateral resolution down to the low- and sub-micrometer scale [75].

In order to test the experimental LMD-ICP-MS arrangement, laser beams from the LMD apparatus with different spot sizes (3–5 μm) were applied either as line scans or in the free-hand modus (spot size 3.5 μm in diameter) to ablate the material from a 30-μm-thick brain tissue with a dried Cu droplet of 6 mm in diameter. Due to the low laser pulse energy, the material was not completely ablated, resulting in relatively lower ion intensities detected by the ICP-MS when compared to that measured by LA-ICP-MS. However, maximum ion intensities of 10^4 cps for $^{63}Cu^+$ can be obtained in each measurement. The variation of ion intensity, especially in the free-hand modus, was due to the inhomogeneous distribution of tissue and Cu, which was verified in LA-ICP-MS measurements. Furthermore, a precise determination of $^{63}Cu/^{65}Cu$ isotope ratios was found in this measurement by LMD-ICP-MS. The limit of detection (LOD) of LMD-ICP-MS for Cu in the 3 μm line scan in the present setup was 190 $\mu g\,g^{-1}$. Due to the fact that the present LMD operated at low laser pulse energy of 1 μJ was not sufficient to ablate all the materials under the pre-set scanning lines, there is a need to improve a more powerful laser beam for applications in imaging with excellent quality. Nevertheless, this low laser energy of LMD was originally designed to cut off the section of interest but also to avoid any damage to the biomolecules. With respect to laser ablation by a picosecond laser with pulse energy >100 mJ in the LMD system, a complete ablation of such a 30 μm-thick tissue section would be possible and subsequently much higher ion intensities and lower LOD would be achievable. Therefore, imaging of elements in biological tissues and cells by improved LMD would be a promising future application with the improvement of spatial resolution and limit of detection for microanalytical investigations on biological samples. Furthermore, based on LMD-ICP-MS, we are proposing to develop a metalloprotein microscope by combining imaging of metals using LMD-ICP-MS and localizing targeted biomolecules using fluorescence staining technique, in order to establish an advanced imaging technique with high spatial resolution for metallomic studies in life sciences.

3. Synchrotron-based micro-X-ray fluorescence and micro-X-ray absorption spectroscopy

Since the last decade of the 20th century, micro-X-ray fluorescence (μ-XRF) has been rapidly developing as one of the newest branches of XRF. Along with the construction of more powerful synchrotron radiation facilities around the world, μ-XRF has become a popular trend in X-ray spectroscopic analysis of small areas. The high energy of the third generation light source ensures enough power of the beam at a level of several keV with a small spot size at the nanometer level. It also allows two-dimensional elemental imaging in biological samples with the advantage of non-destructive measurement at ambient pressure. Various tissues and cells of animals and plants have been scanned using a micro-X-ray beam with a spot size from no larger than 25 μm down to several hundred nanometer [82–84,13,15,25,85,86]. Quite recently, a hard X-ray nanobeam focused in one direction to a width of 7 nm at 20 keV has been achieved at the 1-km-long beamline (BL29XUL) of SPring-8 in Japan, by a laterally graded multilayer mirror used to produce the nanobeam and a grazing-incidence deformable mirror to restore the wavefront shape [87]. The quantification of μ-XRF spectra has also been developed, either, in most cases, based on the analysis of reference materials which have a similar composition and thickness to that of the samples or by performing as standardless quantification if no suitable standards are

available. However, standardless quantification of the μ-XRF spectra is still challenging, since the instrumental parameters such as energy, current and spot size are quite different in different facilities, as well as the fact that the detected fluorescence of each element is dependent on the atomic arrangement in a complex matrix. Biological markers labeled with heavy elements are proposed for the purpose of μ-XRF quantification, especially in the case of the analysis of a single cell, to highlight the visualization of certain cell sub-units and structures [88,89]. Since there is considerable debate about sample preparation by cutting the sample into slices before μ-XRF investigation, with respect to the possible loss and re-distribution of the elements, cryo-scanning μ-XRF was specially designed for cell studies and the sample preparation procedure was improved [90]. Mouse embryonic fibroblast cells were pre-fixed by a quick-freezing technique and then scanned in a well-designed cooling chamber with high vacuum by a focused hard nano X-ray beam (spot size of 30 nm × 50 nm) at a X-ray energy of 11.5 keV. The distributions of K, Ca, Fe, Cu and Zn were successfully visualized and considered to be the real elemental profiles in the cells of the living state. The distributions of these elements (especially those of K, Ca and Fe) differed from those in cells fixed with paraformaldehyde. However, this dedicated instrumentation is hard to achieve at standard beamlines around the world.

Micro-X-ray absorption spectroscopy (μ-XAS) provides precise information on the local chemical environment and geometric structure of a metal species [91–98], as well as of some metalloid (such as As and Se) species [99,100] in the biological tissues and cells with a spatial resolution of around 10 μm, including human cancer cells, single neurons, small regions of brain sections, as well as plant cells and tiny organs. However, the application of μ-XAS to non-metal elements like S in biological samples is relatively rare. Only a few studies have been reported based on bulk XAS analysis, in most cases using the X-ray absorption near edge structure (XANES) to investigate the oxidation state by the identification of certain characteristics, such as small variations of energy at the absorption edge, pre-edge peaks at energies below the principal absorption edge, or peaks after the absorption edge [101,102], since it is practically impossible to obtain extended X-ray absorption fine structure (EXAFS) spectra for the lighter elements (e.g., C and N) [18]. Pickering et al. [99] first obtained quantitative 100-μm-resolution images of specific chemical forms of Se in intact plant tissues by selectively tuning incident X-ray energies close to the Se K-absorption edge. Although XAS and μ-XAS can provide us with considerable information on surroundings of the target atom, including the species and number of the coordination atoms and ligands, the bond length between the central atom and the scattering atoms, and the oxidation state of the central atom, it is generally unable to identify the origin of the ligands. Moreover, in biological samples, the ligands of a certain element may not be a single species, but more often consist of several species, which results in difficulties in spectral analysis, due to the lack of reference spectra for such complicated samples. Unlike the standard preparation in other analytical techniques, it is not appropriate to construct complicated reference materials which are similar to the studied sample according to the information obtained from XAS and μ-XAS spectra and then to use the spectra of the prepared standard to fit the sample spectra, because the metal species in biological systems is not simply a mixture of several chemical compounds, but a symbiosis of a metabolic balance after a long period of evolution. Furthermore, since biological tissues and cells are complex and sophisticated systems, it is difficult to carry out a structure calculation from the XANES spectra like the one commonly used in the studies of physics and materials science. Therefore, to overcome this weakness, chemical analysis of the candidate ligands is necessary and helpful.

The third generation of synchrotron radiation facilities and recent achievements in focusing optics facilitate the application of μ-XRF and μ-XAS in studies of cellular toxicology, metabolism of bio-metals and nano-particles, as well as medicine and pharmacology. However, since access to synchrotron beamlines is limited, considerable attention should be paid to the design and preparation of the experiments. Moreover, data processing and interpretation should be adapted to the analysis of the complex biological system.

4. Raman spectroscopy combined with SNOM

Raman spectroscopy is a well-known spectroscopic technique used to provide chemical information in a sample system through the analysis of the interaction between the illuminating monochromatic light (normally from a laser) and molecular vibrations, phonons or other excitations in the system. However, conventional optical methods like Raman spectroscopy have limitations in spatial resolution with respect to the theoretical optical diffraction limit ($\sim\lambda/2$). This results in a great deal of attention being paid on the improvement of Raman spectroscopy with respect to higher spatial resolution and signal enhancement in a small area of the sample. In the present review, we focus on advanced Raman spectroscopic techniques with the aid of scanning near-field optical microscopic (SNOM) methods.

An aperture SNOM, coupled with surface analytical and spectroscopic methods such as Raman scattering, would permit a high spatial resolution (<100 nm) and a high chemical information content [103]. However, the recorded intensity of Raman scattering drops dramatically to the undetectable range with decreasing aperture size, which was originally designed to increase the spatial resolution. Moreover, since Raman scattering is a small fraction of the scattered light (approximately 1 in 10 million photons) by an excitation, when it is generated from a nano region, the signal would be too weak to be detected separately from the intense Rayleigh scattered laser light. To overcome this weakness, local enhancement of the electromagnetic field is included in the SNOM–Raman scattering measurement.

One of the options is to use surface-enhanced Raman spectroscopy (SERS). SERS is normally carried out on a rough surface made of metal colloid or a substrate containing a certain metal (normally Ag, Au, or Cu). An enhancement in the electric field around the metal can be obtained due to the excitation of the surface plasmons of the metal by the laser, resulting in a significant increase of the Raman scattering by several orders of magnitude [104,105]. The shape of the roughness and the excitation wavelength contribute to the enhancement factor in SERS [106–108]. Using SNOM at high lateral resolution (10 nm), the field distribution close to the surface of gold films has been recorded [109]. The high peaks in the Raman spectra were recorded corresponding to the so-called “hot spots” due to the huge fluctuations of the electromagnetic fields. Therefore, the molecular information on such metal-covered substrates is revealed with high resolution [110]. However, this approach is hard to implement in the study of real biological tissues and cells, because the metal coating of the sample surface may not present the nondestructive cellular information at the level of the organelle structures.

Another approach to enhance Raman scattering is to combine it with an apertureless SNOM, which is known as tip-enhanced Raman spectroscopy (TERS), by enhancing the intensity of laser light using a sharp metallic tip which is brought very close to the sample surface [111], as in the near-field LA-ICP-MS technique. The tip is prepared by either electrochemical etching of a metal wire or evaporating metal nanoparticles on to a suitable material (e.g., atomic force microscopy (AFM) tip [112] or an optical fiber tip [113]). The enhancement of the radiation field is depen-

dent on a combination of the tip material and geometry. Only the molecules located in the vicinity of the tip apex will experience the field enhancement, therefore, providing a highly resolved lateral resolution of approximately the size of the tip apex (20–30 nm) together with the enhanced Raman signal sensitivity down to the single molecule level. Inouye et al. [114] first used a metalized cantilever tip to detect the molecular vibrations with the aid of SERS. Shortly after the success of Inouye et al., Zenobi's group [112] first experimentally demonstrated a TERS applied for the analysis of surface compositions of brilliant cresyl blue and a C60 thin film, with an estimated enhancement factor of more than 2000 and 40,000, respectively, based on the given illuminated area of 300 nm in diameter and a tip diameter of less than 50 nm. Besides organic molecular and material research [115–117], TERS has also been applied in studies of biological tissues and cells [115,118–120]. Hankus et al. [59,113,114] developed a SERS-based nanoimaging probe capable of chemical imaging with nanometer-scale spatial resolution. Each chemical component in sub-cellular environments could be identified in the investigation of bacteria.

TERS is considered a promising technique for imaging of chemical compounds in biological samples with nanoscale lateral resolution. However, Downes et al. [121] observed a limit of 50–100 μW in the illumination power due to a temperature rise of several tens of degrees beneath the tip apex, possibly resulting in the evaporation of water from the tip apex region thus heating-up both the tip and sample while imaging. Malkovskiy et al. [122] also proved that heating depends strongly on the optical properties of the tips and is minimal for laser wavelengths beyond the plasmon resonance of tip. Even at a laser power as low as 1 mW and modest tip enhancement, the magnitude of heating can easily reach 100 K. This is the question that arises with respect to biological samples which are sensitive to the environment, which still requires considerable attention.

5. Conclusion

In this review, we discussed the development and application of analytical techniques in the investigation of biological samples for chemical information with spatial resolution on the low-micrometer and -nanometer scales in the field of life sciences. A big step forward has been made due to the development of the third generation synchrotron radiation facilities so that synchrotron-based techniques such as μ-XRF and μ-XAF are already available for imaging elemental distribution and identifying metal species (at least in the oxidation state) in single cells without destroying the samples. Raman spectroscopy coupled with aperture or apertureless SNOM tips is another frequently used technique to obtain chemical information in organic samples with lateral resolution down to several tens of nanometer, although it is limited in applications for biological samples. Another application of aperture SNOM tip for high spatial resolution is to combine this method with a mass spectrometer. However, the efficiency of this combination is dependent on the sensitivity of the mass analyzer, which results in limited applications for materials with lower analyte concentrations as in the case of a single cell. We propose to use an apertureless Ag tip instead of the optical fiber, and thus the electromagnetic field around the tip can be significantly enhanced due to the near-field enhancement effect. The material ablated by this enhance radiation has proved to be sufficient for identification purposes in the sensitive double-focusing sector-field mass spectrometer. With the near-field LA-ICP-MS developed at Forschungszentrum Jülich, it is possible to analyze biological samples with high spatial resolution in the nanometer range. Further applications of near-field LA-ICP-MS for imaging small biological tissues and single cells will be carried out on a 3D-movement stage operated in the dynamic non-contact feedback mode. In addition, further studies are needed to obtain a better understanding of the physical basis of near-field laser ablation mechanisms as well as to improve performance. On the other hand, apart from using the near-field enhancement effect, it is also possible to directly couple a laser microdissection apparatus to a sensitive mass spectrometer in order to obtain elemental and isotopic information with resolution in the low- and sub-μm range. In the near future, these newly developed techniques will soon open up a window for biochemical studies with high spatial resolution down to the nanometer range in the life sciences.

Acknowledgements

The first author is very grateful for support for this work from the Alexander von Humboldt Foundation. Special thanks are given to Mrs. J. Carter-Sigglow (Zentralbibliothek, Forschungszentrum Jülich) for English correction.

References

[1] J.S. Becker, Inorganic Mass Spectrometry: Principles and Application, John Wiley and Sons, Chichester, 2007.
[2] J.S. Becker, J.Su. Becker, Imaging of metals, metalloids, and non-metals by laser ablation inductively coupled plasma mass spectrometry (LA-ICP-MS) in biological tissues, in: S.S. Rubakhin, J.V. Sweedler (Eds.), Mass Spectrom. Imaging: Princ. Protoc., 2010, pp. 51–82.
[3] J.S. Becker, A. Matusch, C. Palm, D. Salber, K.A. Morton, J.Su. Becker, Bioimaging of metals in brain tissue by laser ablation inductively coupled plasma mass spectrometry (LA-ICP-MS) and metallomics, Metallomics 2 (2010) 104–111.
[4] J.S. Becker, Bioimaging of metals in brain tissue from micrometre to nanometre scale by laser ablation inductively coupled plasma mass spectrometry: state of the art and perspectives, Int. J. Mass Spectrom. 289 (2010) 65–75.
[5] M.L. Heien, P.D. Piehowski, N. Winograd, A.G. Ewing, Lipid detection, identification, and imaging single cells with SIMS, in: S.S. Rubakhin, J.V. Sweedler (Eds.), Mass Spectrometry Imaging: Principles and Protocols, 2010, pp. 85–97.
[6] S.G. Boxer, M.L. Kraft, P.K. Weber, Advances in imaging secondary ion mass spectrometry for biological samples, Annu. Rev. Biophys. 38 (2009) 53–74.
[7] J.S. Becker, U. Breuer, H.-F. Hsieh, T. Osterholt, U. Kumtabtim, B. Wu, Z. Qin, A. Matusch, J.A. Caruso, Bioimaging of metals and biomolecules in mouse heart by laser ablation inductively coupled plasma mass spectrometry (LA-ICP-MS) and secondary ion mass spectrometry (SIMS), Anal. Chem. 82 (2010) 9528–9533.
[8] H. Nygren, P. Malmberg, High-resolution imaging and proteomics of peptide fragments by TOF-SIMS, Proteomics 10 (2010) 1694–1698.
[9] Y. Hsieh, F. Li, W.A. Korfmacher, Mapping pharmaceuticals in rat brain sections using MALDI imaging mass spectrometry, Mass Spectrometry Imaging: Principles and Protocols (2010) 147–158.
[10] D.C. Perdian, S. Cha, J. Oh, D.S. Sakaguchi, E.S. Yeung, Y.J. Lee, In situ probing of cholesterol in astrocytes at the single-cell level using laser desorption ionization mass spectrometric imaging with colloidal silver, Rapid Commun. Mass Spectrom. 24 (2010) 1147–1154.
[11] K.E. Burnum, S.L. Frappier, R.M. Caprioli, Matrix-assisted laser desorption/ionization imaging mass spectrometry for the investigation of proteins and peptides, Annu. Rev. Anal. Chem. 1 (2008) 689–705.
[12] J.Y. Shi, Y.X. Chen, Y.Y. Huang, W. He, SRXRF microprobe as a technique for studying elements distribution in *Elsholtzia splendens*, Micron 35 (2004) 557–564.
[13] M.J. Farquharson, K. Geraki, G. Falkenberg, R. Leek, A. Harris, The localisation and micro-mapping of copper and other trace elements in breast tumours using a synchrotron micro-XRF system, Appl. Radiat. Isotopes 65 (2007) 183–188.
[14] T. Paunesku, S. Vogt, J. Maser, B. Lai, G. Woloschak, X-ray fluorescence microprobe imaging in biology and medicine, J. Cell. Biochem. 99 (2006) 1489–1502.
[15] B. De Samber, R. Evens, K. De Schamphelaere, G. Silversmit, B. Masschaele, T. Schoonjans, B. Vekemans, C.R. Janssen, L. Van Hoorebeke, I. Szalóki, F. Vanhaecke, G. Falkenberge, L. Vincze, A combination of synchrotron and laboratory X-ray techniques for studying tissue-specific trace level metal distributions in Daphnia magna, J. Anal. Atom. Spectrom. 23 (2008) 829–839.
[16] A. Al-Ebraheem, J. Goettlicher, K. Geraki, S. Ralph, M.J. Farquharson, The determination of zinc, copper and iron oxidation state in invasive ductal carcinoma of breast tissue and normal surrounding tissue using XANES, X-ray Spectrom. 39 (2010) 332–337.
[17] I.J Pickering, R.C. Prince, D.E. Salt, G.N. George, Quantitative, chemically specific imaging of selenium transformation in plants, Proc. Natl. Acad. Sci. U. S. A. 97 (2000) 10717–10722.
[18] K. Tsuji, K. Nakano, X-ray Spectrometry, Anal. Chem. 82 (2010) 4950–4987.
[19] C. Petibois, G. Déléris, Chemical mapping of tumor progression by FT-IR imaging: towards molecular histopathology, Trends Biotechnol. 24 (2006) 455–462.

[20] M.K. Kuimova, K.L.A. Chan, S.G. Kazarian, Chemical imaging of live cancer cells in the natural aqueous environment, Appl. Spectrosc. 63 (2009) 164–171.
[21] C.W. Freudiger, W. Min, B.G. Saar, S. Lu, G.R. Holtom, C. He, J.C. Tsai, J.X. Kang, X.S. Xie, Label-free biomedical imaging with high sensitivity by stimulated Raman scattering microscopy, Science 322 (2008) 1857–1861.
[22] M. Kammer, R. Hedrich, H. Ehrlich, J. Popp, E. Brunner, C. Krafft, Spatially resolved determination of the structure and composition of diatom cell walls by Raman and FTIR imaging, Anal. Bioanal. Chem. 398 (2010) 509–517.
[23] J.K. Jaiswal, E.R. Goldman, H. Mattoussi, S.M. Simon, Use of quantum dots for live cell imaging, Nat. Methods 1 (2004) 73–78.
[24] M. Palmieria, C.J. Nowella, M. Condrona, J. Gardinerb, A.B. Holmesb, J. Desaia, A.W. Burgessa, B. Catimel, Analysis of cellular phosphatidylinositol (3,4,5)-trisphosphate levels and distribution using confocal fluorescent microscopy, Anal. Biochem. 406 (2010) 41–50.
[25] G. Sarret, G. Willems, M.-P. Isaure, M.A. Marcus, S.C. Fakra, H. Frérot, S. Pairis, N. Geoffroy, A. Manceau, P. Saumitou-Laprade, Zinc distribution and speciation in Arabidopsis halleri × Arabidopsis lyrata progenies presenting various zinc accumulation capacities, New Phytol. 184 (2009) 581–595.
[26] M.P. Isaure, B. Fayard, G. Saffet, S. Pairis, J. Bourguignon, Localization and chemical forms of cadmium in plant samples by combining analytical electron microscopy and X-ray spectromicroscopy, Spectrochim. Acta B 61 (2006) 1242–1252.
[27] J. Misson, P. Henner, M. Morello, M. Floriani, T.-D. Wu, J.-L. Guerquin-Kern, L. Fevrier, Use of phosphate to avoid uranium toxicity in Arabidopsis thaliana leads to alterations of morphological and physiological responses regulated by phosphate availability, Environ. Exp. Bot. 67 (2009) 353–362.
[28] J.S. Becker, D. Salber, New mass spectrometric tools in brain research, Trends Anal. Chem. 29 (2010) 966–979.
[29] K. Chughtai, R.M.A. Heeren, Mass spectrometric imaging for biomedical tissue analysis, Chem. Rev. 110 (2010) 3237–3277.
[30] R. McRae, P. Bagchi, S. Sumalekshmy, C.J. Fahrni, In situ imaging of metals in cells and tissues, Chem. Rev. 109 (2009) 4780–4827.
[31] L.A. McDonnell, R.M.A. Heeren, Imaging mass spectrometry, Mass Spectrom. Rev. 26 (2007) 606–643.
[32] L.W. Swanson, Liquid metal ion sources: mechanism and applications, Nucl. Instrum. Methods Phys. Res. 218 (1983) 347–353.
[33] R.D. Harris, W.S. Baker, M.J. Van Stipdonk, R.M. Crooks, E.A. Schweikert, Secondary ion yields produced by keV atomic and polyatomic ion impacts on a self-assembled monolayer surface, Rapid Commun. Mass Spectrom. 13 (1999) 1374–1380.
[34] A. Novikov, M. Caroff, S. Della-Negra, J. Depauw, M. Fallavier, Y. Le Beyec, M. Pautrat, J.A. Schultz, A. Tempez, A.S. Woods, The Au_n cluster probe in secondary ion mass spectrometry: influence of the projectile size and energy on the desorption/ionization rate from biomolecular solids, Rapid Commun. Mass Spectrom. 19 (2005) 1851–1857.
[35] P. Sjövall, J. Lausmaa, B. Johansson, Mass spectrometric imaging of lipids in brain tissue, Anal. Chem. 76 (2004) 4271–4278.
[36] G. Slodzian, B. Daigne, F. Girard, F. Boust, F. Hillion, Scanning secondary ion analytical microscopy with parallel detection, Biol. Cell 74 (1992) 43–50.
[37] R.M.A. Heeren, L.A. McDonnell, E. Amstalden, S.L. Luxembourg, A.F.M. Altelaar, S.R. Piersma, Why don't biologists use SIMS? A critical evaluation of imaging MS, Appl. Surf. Sci. 252 (2006) 6827–6835.
[38] S. Chandra, J.F. Chabot, G.H. Morrison, A.C. Leopold, Localization of calcium in amyloplasts of root-cap cells using ion microscopy, Science 11 (1982) 1221–1223.
[39] N. Musat, H. Halm, B. Winterholler, P. Hoppe, S. Peduzzi, F. Hillion, F. Horreard, R. Amann, B.B. Jorgensen, M.M.M. Kuypers, A single-cell view on the ecophysiology of anaerobic phototrophic bacteria, Proc. Natl. Acad. Sci. U. S. A. 105 (2008) 17861–17866.
[40] T. Li, T.D. Wu, L. Mazeas, L. Toffin, J.L. Guerquin-Kern, G. Leblon, T. Bouchez, Simultaneous analysis of microbial identity and function using NanoSIMS, Environ. Microbiol. 10 (2008) 580–588.
[41] K.E. Smart, M.R. Kilburn, C.J. Salter, J.A.C. Smith, C.R.M. Grovenor, NanoSIMS and EPMA analysis of nickel localisation in leaves of the hyperaccumulator plant *Alyssum lesbiacum*, Int. J. Mass Spectrom. 260 (2007) 107–114.
[42] V.I. Slaveykova, C. Guignard, T. Eybe, H.-N. Migeon, L. Hoffmann, Dynamic NanoSIMS ion imaging of unicellular freshwater algae exposed to copper, Anal. Bioanal. Chem. 393 (2009) 583–589.
[43] A.M. Herrmann, P.L. Clode, I.R. Fletcher, N. Nunan, E.A. Stockdale, A.G. O'Donnell, D.V. Murphy, A novel method for the study of the biophysical interface in soils using nano-scale secondary ion mass spectrometry, Rapid Commun. Mass Spectrom. 21 (2007) 29–34.
[44] P.L. Clode, M.R. Kilburn, D.L. Jones, E.A. Stockdale, J.B. Cliff III, A.M. Herrmann, D.V. Murphy, In situ mapping of nutrient uptake in the rhizosphere using nanoscale secondary ion mass spectrometry, Plant Physiol. 151 (2009) 1751–1757.
[45] C. Lechene, F. Hillion, G. McMahon, D. Benson, A.M. Kleinfeld, J.P. Kampf, D. Distel, Y. Luyten, J. Bonventre, D. Hentschel, K.M. Park, S. Ito, M. Schwartz, G. Benichou, G. Slodzian, High-resolution quantitative imaging of mammalian and bacterial cells using stable isotope mass spectrometry, J. Biol. 5 (2006) 20.
[46] C.P. Lechene, Y. Luyten, G. McMahon, D.L. Distel, Quantitative imaging of nitrogen fixation by individual bacteria within animal cells, Science 317 (2007) 1563–1566.
[47] C.R.M. Grovenor, K.E. Smart, M.R. Kilburn, B. Shore, J.R. Dilworth, B. Martin, C. Hawes, R.E.M. Rickaby, Specimen preparation for NanoSIMS analysis of biological materials, Appl. Surf. Sci. 252 (2006) 6917–6924.
[48] D. Touboul, F. Halgand, A. Brunelle, R. Kersting, E. Tallarek, B. Hagenhoff, O. Laprevote, Tissue molecular ion imaging by gold cluster ion bombardment, Anal. Chem. 76 (2004) 1550–1659.
[49] P. Chaurand, K.E. Schriver, R.M. Caprioli, Instrument design and characterization for high resolution MALDI-MS imaging of tissue sections, J. Mass Spectrom. 42 (2007) 476–489.
[50] B. Spengler, M. Hubert, Scanning microprobe matrix-assisted laser desorption ionization (SMALDI) mass spectrometry: instrumentation for sub-micrometer resolved LDI and MALDI surface analysis, J. Am. Soc. Mass Spectrom. 13 (2002) 735–748.
[51] H.R. Aerni, D.S. Cornett, R.M. Caprioli, Automated acoustic matrix deposition for MALDI sample preparation, Anal. Chem. 78 (2006) 827–834.
[52] W. Bouschen, B. Spengler, Artifacts of MALDI sample preparation investigated by high-resolution scanning microprobe matrix-assisted laser desorption/ionization (SMALDI) imaging mass spectrometry, Int. J. Mass Spectrom. 266 (2007) 129–137.
[53] J.C. Jurchen, S.S. Rubakhin, J.V. Sweedler, MALDI-MS imaging of features smaller than the size of the laser beam, J. Am. Soc. Mass Spectrom. 16 (2005) 1654–1659.
[54] S. Guenther, M. Koestler, O. Schulz, B. Spengler, Laser spot size and laser power dependence of ion formation in high resolution MALDI imaging, Int. J. Mass Spectrom. 294 (2010) 7–15.
[55] A. Vertes, M. Reeves, F. Kashanchi, Protein Microscope, PCT, WO, 2006/081240 A1.
[56] D.W. Pohl, W. Denk, M. Lanz, Optical stethoscopy: image recording with resolution λ/20, Appl. Phys. Lett. 44 (1984) 651–653.
[57] U. Dürig, D.W. Pohl, F. Rohner, Near-field optical-scanning microscopy, J. Appl. Phys. 59 (1986) 3318–3327.
[58] E. Betzig, J.K. Trautman, T.D. Harris, J.S. Weiner, R.L. Kostelak, Breaking the diffraction barrier: optical microscopy on a nanometric scale, Science 251 (1991) 1468–1470.
[59] M.E. Hankus, G. Gibson, N. Chandrasekharan, B.M. Cullum, Surface-enhanced Raman scattering (SERS)-nanoimaging probes for biological analysis, SPIE Proc. 5588 (2004) 106–116.
[60] R. Gallacchi, S. Koèlsch, H. Kneppe, A.J. Meixner, Well-shaped fibre tips by pulling with a foil heater, J. Microsc. 202 (2001) 182–187.
[61] R. Stöckle, C. Fokas, V. Deckert, R. Zenobi, B. Sick, B. Hecht, U.P. Wild, High-quality near-field optical probes by tube etching, Appl. Phys. Lett. 75 (1999) 160–162.
[62] Y.D. Suh, R. Zenobi, Improved probes for scanning near-field optical microscopy, Adv. Mater. 12 (2000) 1139–1142.
[63] D. Zeisel, S. Nettesheim, B. Dutoit, R. Zenobi, Pulsed laser-induced desorption and optical imaging on a nanometer scale with scanning near-field microscopy using chemically etched fiber tips, Appl. Phys. Lett. 68 (1996) 2491–2492.
[64] D.A. Kossakovski, S.D. O'Connor, M. Widmer, J.D. Baldeschwieler, J.L. Beauchamp, Spatially resolved chemical analysis with an NSOM-based laser desorption microprobe, Ultramicroscopy 71 (1998) 111–115.
[65] R. Stöckle, P. Setz, V. Deckert, T. Lippert, A. Wokaun, R. Zenobi, Nanoscale atmospheric pressure laser ablation-mass spectrometry, Anal. Chem. 73 (2001) 1399–1402.
[66] P.D. Setz, T.A. Schmitz, R. Zenobi, Design and performance of an atmospheric pressure sampling interface for ion-trap/time-of-flight mass spectrometry, Rev. Sci. Instrum. 77 (2006) 024101.
[67] T.A. Schmitz, G. Gamez, P.D. Setz, L. Zhu, R. Zenobi, Towards nanoscale molecular analysis at atmospheric pressure by a near-field laser ablation ion trap/time-of-flight mass spectrometer, Anal. Chem. 80 (2008) 6537–6544.
[68] L. Zhu, G. Gamez, T.A. Schmitz, F. Krumeich, R. Zenobi, Material ejection and redeposition following atmospheric pressure near-field laser ablation on molecular solids, Anal. Bioanal. Chem. 396 (2010) 163–172.
[69] J.S. Becker, M. Kayser, A. Gorbunoff, W. Pompe, G. Roedel, U. Krause-Buchholz, M. Przybylski, Verfahren und Vorrichtung zur Durchführung einer ortsaufgelösten Lokal- und Verteilungsanalyse und zur quantitativen Bestimmung von Elementkonzentrationen, German Patent, 2008 (November 2003).
[70] J.S. Becker, A. Gorbunoff, M. Zoriy, A. Izmer, M. Kayser, Evidence of near-field laser ablation inductively coupled plasma mass spectrometry (NF-LA-ICP-MS) at nanometre scale for elemental and isotopic analysis on gels and biological samples, J. Anal. Atom. Spectrom. 21 (2006) 19–25.
[71] M.V. Zoriy, M. Kayser, J.S. Becker, Possibility of nano-local element analysis by near-field laser ablation inductively coupled plasma mass spectrometry (LA-ICP-MS): new experimental arrangement and first application, Int. J. Mass Spectrom. 273 (2008) 151–155.
[72] M.V. Zoriy, J.S. Becker, Near-field laser ablation inductively coupled plasma mass spectrometry: a novel elemental analytical technique at the nanometer scale, Rapid Commun. Mass Spectrom. 23 (2009) 23–30.
[73] M.V. Zoriy, D. Mayer, J.S. Becker, Metal imaging on surface of micro- and nanoelectronic devices by laser ablation inductively coupled plasma mass spectrometry and possibility to measure at nanometer range, J. Am. Soc. Mass Spectrom. 20 (2009) 883–890.
[74] J.S. Becker, D. Salber, Method and device for carrying out a quantitative spatially resolved local distribution analysis of chemical elements and in-situ characterization of the ablated surface regions. Patent (8.4.2009) WO2010115394 A1 granted Dec. 2010.

[75] J.S. Becker, S. Niehren, A. Matusch, B. Wu, H.-F. Hsieh, U. Kumtabtim, M. Hamester, A. Plaschke-Schlütter, D. Salber, Scaling down the bioimaging of metals by laser microdissection inductively coupled plasma mass spectrometry (LMD-ICP-MS), Int. J. Mass Spectrom. 294 (2010) 1–6.
[76] A.I. De Souza, E. McGregor, M.J. Dunn, M.L. Rose, Preparation of human heart for laser microdissection and proteomics, Proteomics 4 (2004) 578–586.
[77] A. Vogel, K. Lorenz, V. Horneffer, G. Hüttmann, D. von Smolinski, A. Gebert, Mechanisms of laser-induced dissection and transport of histologic specimens, Biophys. J. 93 (2007) 4481–4500.
[78] M.R. Emmert-Buck, R.F. Bonner, P.D. Smith, R.F. Chuaqui, Z. Zhuang, S.R. Goldstein, R.A. Weiss, L.A. Liotta, Laser capture microdissection, Science 274 (1996) 998–1001.
[79] V. Espina, M. Heiby, M. Pierobon, L.A. Liotta, Laser capture microdissection technology, Expert Rev. Mol. Diagn. 7 (2007) 647–657.
[80] G. Ernst, C. Melle, B. Schimmel, A. Bleul, F. von Eggeling, Proteohistography – direct analysis of tissue with high sensitivity and high spatial resolution using ProteinChip technology, J. Histochem. Cytochem. 54 (2006) 13–17.
[81] R.W. Hutchinson, A.G. Cox, C.W. McLeod, P.S. Marshall, A. Harper, E.L. Dawson, D.R. Howlett, Imaging and spatial distribution of β-amyloid peptide and metal ions in Alzheimer's plaques by laser ablation-inductively coupled plasma-mass spectrometry, Anal. Biochem. 346 (2005) 225–233.
[82] A. Ide-Ektessabi, T. Kawakami, F. Watt, Distribution and chemical state analysis of iron in the Parkinsonian substantia nigra using synchrotron radiation micro beams, Nucl. Instrum. Methods 213 (2004) 590–594.
[83] M. Szczerbowska-Boruchowska, J. Chwiej, M. Lankosz, D. Adamek, S. Wojcik, A. Krygowska-Wajs, B. Tomik, S. Bohic, J. Susini, A. Simionovici, P. Dumas, M. Kastyak, Intraneuronal investigations of organic components and trace elements with the use of synchrotron radiation, X-ray Spectrom. 34 (2005) 514–520.
[84] M.-P. Isaure, B. Fayard, G. Sarret, S. Pairis, J. Bourguignon, Localization and chemical forms of cadmium in plant samples by combining analytical electron microscopy and X-ray spectromicroscopy, Spectrochim. Acta B 61 (2006) 1242–1252.
[85] F. Liang, G.L. Zhang, X.L. Xiao, Z.H. Cai, B. Lai, Y. Hwuc, C.H. Yan, J. Xu, Y.L. Li, M.G. Tan, C.F. Zhang, Y. Li, Toxicological study of injuries of rat's hippocampus after lead poisoning by synchrotron microradiography and elemental mapping, Nucl. Instrum. Methods 268 (2010) 2840–2845.
[86] E. Harada, A. Hokura, S. Takada, K. Baba, Y. Terada, I. Nakai, K. Yazaki, Characterization of cadmium accumulation in willow as a woody metal accumulator using synchrotron radiation-based X-ray microanalyses, Plant Cell Physiol. 51 (2010) 848–853.
[87] H. Mimura, S. Handa, T. Kimura, H. Yumoto, D. Yamakawa, H. Yokoyama, S. Matsuyama, K. Inagaki, K. Yamamura, Y. Sano, K. Tamasaku, Y. Nishino, M. Yabashi, T. Ishikawa, K. Yamauchi, Breaking the 10 nm barrier in hard-X-ray focusing, Nat. Phys. 6 (2010) 122–125.
[88] S. Corezzi, L. Urbanelli, P. Cloetens, C. Emiliani, L. Helfen, S. Bohic, F. Elisei, D. Fioretto, Synchrotron-based X-ray fluorescence imaging of human cells labeled with CdSe quantum dots, Anal. Biochem. 388 (2009) 33–39.
[89] R. McRae, B. Lai, S. Vogt, C.J. Fahrni, Correlative microXRF and optical immunofluorescence microscopy of adherent cells labeled with ultrasmall gold particles, J. Struct. Biol. 155 (2006) 22–29.
[90] S. Matsuyama, M. Shimura, M. Fujii, K. Maeshima, H. Yumoto, H. Mimura, Y. Sano, M. Yabashi, Y. Nishino, K. Tamasaku, Y. Ishizaka, T. Ishikawa, K. Yamauchi, Elementalmapping of frozen-hydrated cells with cryo-scanning X-ray fluorescence microscopy, X-ray Spectrom. 39 (2010) 260–266.
[91] C.M. Hansel, M.J. La Force, S. Fendorf, S. Sutton, Spatial and temporal association of As and Fe species on aquatic plant roots, Environ. Sci. Technol. 36 (2002) 1988–1994.
[92] J.A. Howe, R.H. Loeppert, V.J. DeRose, D.B. Hunter, P.M. Bertsch, Localization and speciation of chromium in subterranean clover using XRF, XANES, and EPR spectroscopy, Environ. Sci. Technol. 37 (2003) 4091–4097.
[93] G. Sarret, J. Balesdent, L. Bouziri, J.M. Garnier, M.A. Marcus, N. Geoffroy, F. Panfili, A. Manceau, Zn speciation in the organic horizon of a contaminated soil by micro-X-ray fluorescence, micro- and powder-EXAFS spectroscopy, and isotopic dilution, Environ. Sci. Technol. 38 (2004) 2792–2801.
[94] A. Levina, C.T. Dillon, I. Mulyani, B. Lai, Z.H. Cai, P.A. Lay, Time-dependent uptake, distribution and biotransformation of chromium(VI) in individual and bulk human lung cells: application of synchrotron radiation techniques, J. Biol. Inorg. Chem. 10 (2005) 105–118.
[95] M.D. Hall, C.T. Dillon, M. Zhang, P. Beale, Z.H. Cai, B. Lai, A.P.J. Stampfl, T.W. Hambley, The cellular distribution and oxidation state of platinum(II) and platinum(IV) antitumour complexes in cancer cells, J. Biol. Inorg. Chem. 8 (2003) 726–732.
[96] S. Yoshida, A. Ektessabi, S. Fujisawa, XANES spectroscopy of a single neuron from a patient with Parkinson's disease, J. Synchrotron Radiat. 8 (2001) 998–1000.
[97] J. Chwiej, D. Adamek, M. Szczerbowska-Boruchowska, A. Krygowska-Wajs, S. Wojcik, G. Falkenberg, A. Manka, M. Lankosz, Investigations of differences in iron oxidation state inside single neurons from substantia nigra of Parkinson's disease and control patients using the micro-XANES technique, J. Biol. Inorg. Chem. 12 (2007) 204–211.
[98] E. Lombi, K.G. Scheckel, J. Pallon, A.M. Carey, Y.G. Zhu, A.A. Meharg, Speciation and distribution of arsenic and localization of nutrients in rice grains, New Phytol. 184 (2009) 193–201.
[99] I.J. Pickering, R.C. Prince, D.E. Salt, G.N. George, Quantitative, chemically specific imaging of selenium transformation in plants, Proc. Natl. Acad. Sci. U. S. A. 97 (2000) 10717–10722.
[100] I.J. Pickering, R.C. Prince, M.J. George, R.D. Smith, G.N. George, D.E. Salt, Reduction and coordination of arsenic in Indian mustard, Plant Physiol. 122 (2000) 1171–1178.
[101] F. Jalilehvand, Sulfur: not a 'silent' element any more, Chem. Soc. Rev. 35 (2006) 1256–1268.
[102] H.R. Lin, J.Y. Shi, B. Wu, J.J. Yang, Y.X. Chen, Y.D. Zhao, T.D. Hu, Speciation and biochemical transformations of sulfur and copper in rice rhizosphere and bulk soil—XANES evidence of sulfur and copper associations, J. Soil Sediment 10 (2010) 907–914.
[103] D. Zeisel, B. Dutoit, V. Deckert, T. Roth, R. Zenobi, Optical spectroscopy and laser desorption on a nanometer scale, Anal. Chem. 69 (1997) 749–754.
[104] M. Fleischmann, P.J. Hendra, A.J. McQuillan, Raman spectra of pyridine adsorbed at a silver electrode, Chem. Phys. Lett. 26 (1974) 163–166.
[105] D.L. Jeanmaire, R.P. van Duyne, Surface Raman spectroelectrochemistry. Part I. Heterocyclic, aromatic, and aliphatic amines adsorbed on the anodized silver electrode, J. Electroanal. Chem. 84 (1977) 1–20.
[106] S. Hayashi, T. Konishi, Scanning near-field optical microscopic observation of surface-enhanced Raman scattering mediated by metallic particle-surface gap modes, Jpn. J. Appl. Phys. 44 (2005) 5313–5318.
[107] S. Buil, J. Aubineau, J. Laverdant, X. Quelin, Local field intensity enhancements on gold semicontinuous films investigated with an aperture nearfield optical microscope in collection mode, J. Appl. Phys. 100 (2006) 063530–63535.
[108] J. Laverdant, S. Buil, X. Quelin, Local field enhancements on gold and silver nanostructures for aperture near field spectroscopy, J. Lumin. 127 (2007) 176–180.
[109] S. Gresillon, J.C. Rivoal, P. Gadenne, X. Quelin, V. Shalaev, A. Sarychev, Nanoscale observation of enhanced electromagnetic field, Phys. Status Solidi A 175 (1999) 337–343.
[110] V. Deckert, D. Zeisel, R. Zenobi, T. Vo-Dinh, Near-field surface-enhanced Raman imaging of dye-labeled DNA with 100-nm resolution, Anal. Chem. 70 (1998) 2646–2650.
[111] J. Wessel, Surface-enhanced optical microscopy, J. Opt. Soc. Am. B 2 (1985) 1538–1541.
[112] R. Stöckle, Y. Suh, V. Deckert, R. Zenobi, Nanoscale chemical analysis by tip-enhanced Raman spectroscopy, Chem. Phys. Lett. 318 (2000) 131–136.
[113] M.E. Hankus, B.M. Cullum, SERS probes for the detection and imaging of biochemical species on the nanoscale, SPIE Proc. 6380 (2006) U23–U34.
[114] Y. Inouye, N. Hayazawa, K. Hayashi, Z. Sekkat, S. Kawata, Near-field scanning optical microscope using a metallized cantilever tip for nanospectroscopy, SPIE Proc. 3791 (1999) 40–48.
[115] B. Pettinger, B. Ren, G. Picardi, R. Schuster, G. Ertl, Nanoscale probing of adsorbed species by tip-enhanced Raman spectroscopy, Phys. Rev. Lett. 92 (2004) 96101.
[116] C.C. Neacsu, J. Dreyer, N. Behr, M.B. Raschke, Scanning-probe Raman spectroscopy with single-molecule sensitivity, Phys. Rev. B 73 (2006) 193406.
[117] W.H. Zhang, T. Schmid, B.S. Yeo, R. Zenobi, Tip-enhanced Raman spectroscopy reveals rich nanoscale adsorption chemistry of 2-mercaptopyridine on Ag, Isr. J. Chem. 47 (2007) 177–184.
[118] M.E. Hankus, B.M. Cullum, SERS nanoimaging probes for characterizing extracellular surfaces, SPIE Proc. 6759 (2007) 75908–175908.
[119] D. Cialla, T. Deckert-Gaudig, C. Budich, M. Laue, R. Mçller, D. Naumann, V. Deckert, J. Popp, Raman to the limit: tip-enhanced Raman spectroscopic investigations of a single tobacco mosaic virus, J. Raman Spectrosc. 40 (2009) 240–243.
[120] U. Neugebauer, U. Schmid, K. Baumann, W. Ziebuhr, S. Kozitskaya, V. Deckert, M. Schmitt, J. Popp, Towards a detailed understanding of bacterial metabolism—spectroscopic characterization of Staphylococcus epidermidis, Chem. Phys. Chem. 8 (2007) 124–137.
[121] A. Downes, R. Mouras, M. Mari, A. Elfick, Optimising tip-enhanced optical microscopy, J. Raman Spectrosc. 40 (special issue) (2009) 1355–1360.
[122] A.V. Malkovskiy, V.I. Malkovsky, A.M. Kisliuk, C.A. Barrios, M.D. Foster, A.P. Sokolov, Tip-induced heating in apertureless near-field optics, J. Raman Spectrosc. 40 (2009) 1349–1354.